Journal of Archaeological Science: Reports 29 (2020) 102181

Contents lists available at ScienceDirect

Journal of Archaeological Science: Reports

journal homepage: www.elsevier.com/locate/jasrep

# Using dental enamel to uncover the impact of childhood diet on mortality in Petra, Jordan

Megan A. Perry[a,*], Mallory Provan[a], Robert H. Tykot[b], Laurel M. Appleton[c], Alysha J. Lieurance[d]

[a] Department of Anthropology, East Carolina University, Greenville, NC 27858 USA
[b] Department of Anthropology, University of South Florida, Tampa, FL 33620 USA
[c] Department of Alumni Relations, Dartmouth College, Hanover, NH 03781 USA
[d] Department of Anthropology, University of Pittsburgh, Pittsburgh, PA 15260 USA

ARTICLE INFO

*Keywords:*
Carbon isotopes
Oxygen isotopes
Diet
Childhood
Petra

ABSTRACT

Isotopic investigations of diet can provide unique perspectives into food acquisition in addition to dietary choices and shifts through the human life course. Here we examine childhood diet at first century B.C. and first century A.D. Petra through carbon and oxygen isotope ratios ($\delta^{13}C$ and $\delta^{18}O$) in dental enamel apatite. Isotope values from the first molars (n = 31), first premolars (n = 20), and second molars (n = 29) were compared to track dietary shifts and characterize water sources from birth until approximately 7 years of age. These isotope values also were assessed by age-at-death to outline the life history impacts of childhood feeding strategies. The childhood diet at Petra generally contained a higher contribution of $C_4$ sources than adults, represented by 29 bone apatite samples, although the level of this contribution and/or the age they were incorporated and removed from the childhood diet varied greatly within the sample. Similarly, heterogeneity in $\delta^{18}O$ across tooth classes seems to reflect variation in water source and potential heat alteration rather than a mother-infant isotopic offset. However, these different strategies did not contribute to varied childhood mortality.

## 1. Introduction

Bioarchaeologists often use childhood disease and nutrition patterns as measures of overall population adaptability to the environment (Goodman and Armelagos, 1988; Katzenberg et al., 1996; Lewis, 2007). Fetal and infant nutrition levels and infectious disease burdens can have lasting impact later in life and even into successive generations (Gluckman et al., 2005; Jang and Serra, 2014; Tomori et al., 2017; Victora et al., 2016). The weaning period, marked by a shift in dietary sources and altered immune functioning, represents a particularly vulnerable age for growth and development in childhood. Stable isotopes in bone and dentin collagen can be used to identify when dietary shifts associated with weaning occur. However, taphonomic factors can often result in poor collagen preservation, hindering isotope analysis using this organic material. In addition, underrepresentation of infants in a skeletal sample prohibits the use of bone collagen to track weaning changes. Here we explore isotopic reflections of childhood diet shifts and mother-infant isotopic offsets associated with weaning using the mineral component of dental enamel from one community within the ancient urban city of Petra, the political and economic center of the Nabataean kingdom (Fig. 1). Preliminary investigations of skeletal lesions related to disease and physiological stress (Canipe, 2014) in addition to age-related mortality patterns (Propst and Perry forthcoming) in adults from this neighborhood suggests they had little exposure to conditions leading to skeletal lesions besides those causing degenerative joint disease and their hazard of death increased much later in the lifespan than expected. We seek to identify potentially culturally-mediated childhood diet patterns that reduced childhood risk and potentially impacted adult frailty.

## 2. Background

### 2.1. Investigating childhood diet through isotope analysis

The timing of weaning and nature of food supplementation during infancy can profoundly impact morbidity and mortality during childhood (Gowland, 2015; Halcrow and Tayles, 2008, 2011; Halcrow et al., 2017; Lewis, 2007). Human breastmilk provides essential nutrients for this stage of childhood development and transmits immunoglobulins protecting the baby from infection. Weaning too early may leave the

* Corresponding author.
*E-mail addresses:* perrym@ecu.edu (M.A. Perry), provanm16@students.ecu.edu (M. Provan), rtykot@usf.edu (R.H. Tykot), laurel.m.appleton@dartmouth.edu (L.M. Appleton), ajl127@pitt.edu (A.J. Lieurance).

https://doi.org/10.1016/j.jasrep.2019.102181
Received 17 April 2019; Received in revised form 11 November 2019; Accepted 18 December 2019

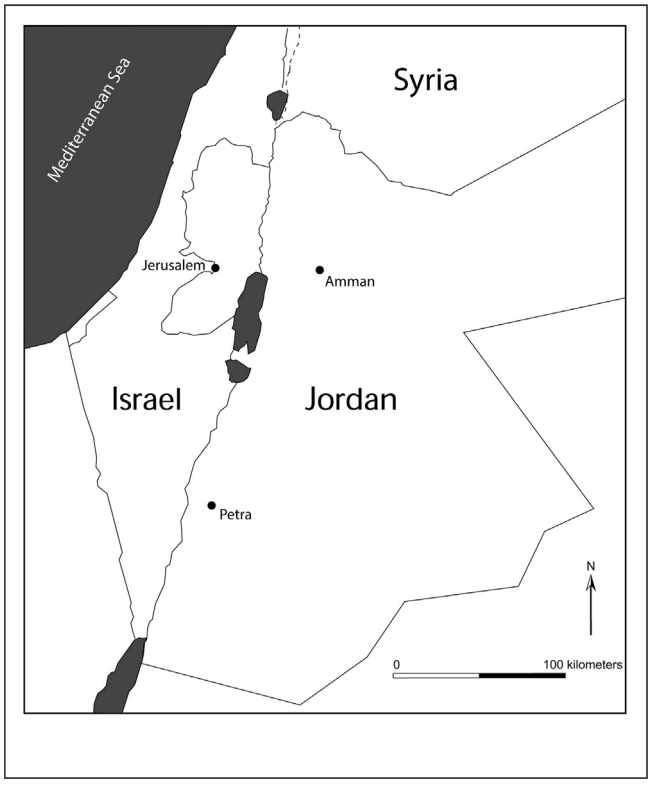


**Fig. 1.** Map showing the location of Petra.

infant more susceptible to infection and unable to absorb nutrients from other foods, and thus the age weaning commences has a significant impact on morbidity and mortality (Katzenberg et al., 1996; WHO, 2003; Pearson et al., 2010). The weaning process itself introduces new bacteria and potential parasites with the introduction of solid foods to children without fully developed immune systems. Only limited types of foods may be introduced during weaning, possibly resulting in deficiencies in vitamins and minerals necessary during this period of growth and development.

Stable isotopes have provided the best indication of dietary changes and mother-infant isotopic offsets that occur with weaning in ancient communities. Typically, investigations into weaning utilize $\delta^{13}C$ and $\delta^{15}N$ ratios extracted from bone collagen from skeletons across age classes or incremental analysis of dentin collagen to track the reduction of breastfeeding and a relative change in $C_3$ and $C_4$ plant sources with the introduction of solid food (Fuller et al., 2006; King et al., 2017; Schurr, 1998; Dupras et al., 2001; Mays, 2010; Richards et al., 2002; Tsutaya and Yoneda, 2015). Incremental sampling of dentin provides the soundest reflection of weaning-related changes (Beaumont et al., 2013, 2018; King et al., 2017). Skeletal turnover rates vary throughout childhood, and thus bone collagen of children from different ages reflects diet during varied periods of time before death (Matsubayashi and Tayasu, 2019; Tsutaya and Yoneda, 2013). In addition, characterizing childhood diet based on those dying during childhood presents a strong mortality bias of the results (Wood et al., 1992). Furthermore, aggregation of bone samples from different children do not reflect individual-level changes occurring through childhood, which masks heterogeneity in the sample that could differentially impact childhood frailty (Kendall, 2016; King et al., 2017). Finally, dentin stable isotope values can be elevated during periods of physiological stress (Beaumont et al., 2018).

Many taphonomic and cultural factors can inhibit the study of childhood diet using collagen in either bone or dentin. Stable isotope analysis of bone collagen requires an adequate cross-section of children dying during childhood and analysis of either bone or dentin necessitates adequate collagen preservation. Numerous factors impact preservation of collagen, including exposure to microbial environments, soil acidity and temperature, and hydrology (DeNiro, 1985; Harbeck and Grupe, 2009; Hedges, 2002; Hedges and Millard, 1995; Tuross, 2002; Weiner and Bar-Yosef, 1990). The underrepresentation of children can result from either differential burial by age or poor preservation of relatively porous infant remains (Gordon and Buikstra, 1981; Guy et al., 1997; Walker et al., 1988).

Dental enamel provides an alternative source of dietary information, which like dentin remains unchanged since childhood development but generally is less susceptible to diagenetic change than bioapatite in bone or dentin (Budd et al., 2000; Lee-Thorp and Sponheimer, 2003). Bone apatite may provide comparative data on the adult diet in cases of poor collagen preservation, although the lack of preserved collagen may be associated with decreased preservation of bone minerals (Hedges, 2002). Although bulk dental enamel samples cannot provide a detailed weaning scenario, intra-tooth comparisons can be used to track general dietary changes through childhood as well as within-individual shifts that may be related to weaning and measure the impact of childhood dietary composition on the life history of individuals.

### 2.2. Expectations and limitations of using bulk enamel samples at Petra

The human remains recovered from the tombs on the North Ridge in Petra fall into the categories of infant underrepresentation and inadequate collagen preservation. The skeletal assemblage derives from five tombs (B.4, B.5, B.6, B.7, and F.1) excavated between 2012 and 2016 by the Petra North Ridge Project (PNRP) (Parker and Perry, 2013, 2017; Perry 2017, Perry and Walker, 2018). In addition, bones from Tomb 2 excavated in an earlier phase of the PNRP in 1999 (Bikai and Perry, 2001) were included in the analysis. The Petra North Ridge was used as a cemetery between the 2nd century BCE and the turn of the 2nd century CE While Petra is known for its elaborately-carved façade tombs that surround the city center, these tombs consist of more simple rectangular chambers accessed through shafts cut vertically into the exposed bedrock. A combination of natural processes, tomb looting, and mortuary behaviors have caused the commingling and fragmentation of the majority of the skeletal remains.

The Petra North Ridge sample contains a small proportion of individuals under 18 years of age, only 20 of a total MNI of 121. In addition, almost all of these are over the suspected age of weaning based textual evidence and other isotopic studies of weaning from this temporal and geographic context (e.g., Bourbou and Garvie-Lok, 2009; Dupras and Tocheri, 2007). The sieving of burial deposits at Petra and the relatively good preservation of subadult bones that do exist may indicate that differential burial of infants and children, rather than taphonomic factors, has caused this deficit (see Saunders, 1992). Preservation of collagen molecules also is a fundamental issue in the Petra North Ridge sample. Preliminary carbon and nitrogen isotope analysis of 34 human bone samples from Petra found that only eight had a C:N ratio falling within the recommended interval of 2.9 and 3.6 (DeNiro, 1985).

The mineral density of dental enamel often prevents significant diagenetic contamination beyond the crown surface (Budd et al., 2000; Hoppe et al., 2003; Lee-Thorp and Sponheimer, 2003) and can be used in place of dentin in cases of poor collagen preservation. The analysis of dental enamel, similar to dentin, ameliorates the mortality bias created by analyzing a sample of deceased children (e.g., Beaumont et al., 2015) by including all individuals living beyond the age that tooth formation began. However, the bulk sampling of dental enamel combines the isotopes consumed throughout its formation, creating difficulty in tracking the exact year weaning began and ended. Instead, this method can be used to track general dietary changes over childhood, illuminate possible dietary heterogeneity, as well as identify a relationship between childhood morbidity and mortality and diet. This

study analyzed $\delta^{13}C$ and $\delta^{18}O$ stable isotope ratios in enamel carbonate from teeth forming at different ages during childhood: the permanent first molar with a crown forming from birth to 2.8 years, the first premolar that forms between 2.5 and 6.4 years, and the second molar that forms from 3.7 to 7.4 years (Moorees et al., 1963; Šešelj et al. 2019). These three teeth thus span the likely period of weaning, and despite the slight overlap, can track dietary changes occurring during their crown development (Dupras and Tocheri, 2007; Wright and Schwarcz, 1998, 199; Wright, 2013; Tsutaya and Yoneda, 2015). In addition, bone apatite from adults was used to represent the general adult diet for comparison to the children's values. Bone collagen $\delta^{13}C$ provides a dietary signal that reflects mainly consumed protein whereas $\delta^{13}C$ in enamel reflects the carbon dietary mix of lipids, proteins, and carbohydrates (Krueger and Sullivan, 1984; Lee-Thorp et al., 1989; Tykot, 2004, 2014).

Oxygen isotopes in dental carbonate reflect sources of ingested water (Luz et al., 1984), and there is an isotopic offset of approximately 1‰ between an infant receiving their water through human breastmilk versus through direct consumption of environmental water (Wright and Schwarcz, 1998). Archaeologists also use $\delta^{18}O$ to assess population mobility by comparing the dental enamel value to that expected based on local water sources where they died (Dupras and Schwarcz, 2001; Perry et al., 2009; Prowse et al., 2007; Wright and Schwarcz, 1999). Alteration of water through exposure to heat (Brettell et al., 2012; Daux et al., 2008; Tuross et al., 2017), fermentation (in the case of water in grapes or grains; Akamatsu et al., 2019; Brettell et al., 2012), or catchment and storage practices (Gat and Dansgaard, 1972) can shift $\delta^{18}O$ more than the 1‰ seen in weaning, potentially masking or enhancing any mother-infant isotopic offset. Supplementing or replacing human breastmilk with that from animals also would confound interpretations of weaning from $\delta^{18}O$ (Daux et al., 2008).

### 2.3. Exploring the impact of childhood diet on life history

Assessing childhood diet within this sample would highlight factors that may have impacted the life history of the individuals within one neighborhood in Petra during a period of increased urbanization and prosperity. This structural change is exemplified by construction of monumental and civic structures, elaborate urban villas, and the carving of monumental tomb facades (Schmid, 2002). Petra's impressive built hydraulic infrastructure mitigated the area's semi-arid climate and not only provided water for city inhabitants, but also to agricultural fields in the city's environs (Beckers et al., 2013; Ortloff, 2005). Paleobotanical evidence indicates that grains such as wheat and barley in addition to fruits such as grapes and figs, nuts, and legumes were grown in the region during this period and these $C_3$ plants presumably were consumed by the city's residents (Bouchaud, 2015; Ramsay and Bedal, 2015). Evidence for the $C_4$ plant millet exists in the region but at frequencies much smaller than the other plant products (Ramsay and Bedal, 2015; Ramsay and Smith, 2013), and while sorghum could have been grown in the region it does not preserve well in the archaeological record. Sheep, goats, and chickens make up the primary source of meat and animal byproducts based on zooarchaeological evidence (Studer, 2007), and element representation, age and sex distribution, and butchery patterns indicate herd animals were bought whole and slaughtered in the domestic context rather than purchasing pre-butchered pieces, but they were raised outside of the city.

The paleobotanical and zooarchaeological evidence suggests that children at Petra likely would be fed primarily $C_3$ solid food sources, examples of which can be derived from textual sources. Ancient writers such as Soranus of Ephesus (1st century CE; Soranus trans. by Temkin 1991) and Oribasius of Pergamon (writing in the 4th century CE but borrowing heavily from the 2nd century CE physician Galen; Laskaratos and Poulakou-Rebdakau, 2003), all born in the eastern Mediterranean region and educated in Alexandria, suggest what foods should be used to supplement breastmilk during weaning and when weaning should occur. The incorporation of Greco-Roman medical precepts by the Nabataean public cannot be assumed, but the artistic and architectural connections between Petra and Alexandria and the influence of Hellenism in Nabataean society may suggest either an adoption of some precepts or that the writings reflected common practice. Soranus (Book II:17–18) indicates that human breastmilk can come from a mother or wet nurse during breastfeeding, occasionally mixed with honey or goat's milk. Foods such as honey, spelt, eggs, gruel, and pap (a mixture of flour and bread cooked in water) should gradually be used to supplement milk during weaning. Weaning should start when the body becomes "solid" (usually at least 6 months of age) and continue until 3 years of age.

The dental enamel isotope data were integrated with other bioarchaeological data to identify longer-term effects of the infant diet. Whether dietary differences led to increased mortality during childhood was identified by comparing isotope values of the first permanent molars (which includes the critical breastfeeding, weaning, and post-weaning periods) between the subadults, identified by an incompletely formed M1 or a completely formed M1 with little to no attrition, and the adults, identified by complete M1 formation and at least moderate attrition. While the attrition indicator assumes similar abrasives in food across the sample, it allowed inclusion of individuals slightly older than approximately 10 years of age, when the M1 root apex closes, in the subadult category (Moorees et al., 1963; Šešelj et al., 2019). The association between childhood stress and weaning also was examined at Petra through identifying the age of formation of enamel hypoplastic defects. These defects are furrows or indentations that appear in the enamel of a tooth crown as a result of physiological stress during enamel formation (Hillson, 2014). Hypoplastic defects have a multifactorial etiology, but usually result from malnutrition, very acute, severe illnesses, or physical injury that causes a reduction in enamel deposition (Masterson et al., 2017). Age of defect occurrence in the dentition can be estimated using a decile approach that takes into consideration non-linear growth trajectories of dental enamel (Reid and Dean 2000, 2006), or for the incisors and canines, exponential regression formulae developed from Reid and Dean's approach (Henriquez and Oxenham, 2019). However, samples with notable dental attrition prevent identifying the original crown height needed for decile estimation, and in those cases a more traditional linear regression (e.g., Goodman and Rose, 1990) should be used.

## 3. Materials and methods

### 3.1. Materials

The PNRP sample contains the skeletal remains of at least 121 individuals based on a modified feature-based recording database created in FileMaker 14.0 by Anna Osterholtz (2019). The overall PNRP dental sample contains 82 permanent first premolars, 140 permanent first molars, and 137 permanent second molars, some of which were in occlusion and others still under formation. This isotopic study included 29 human adult bone samples from three tombs (Tomb 2, Tomb B.4, and Tomb B.5) for $\delta^{13}C$ analysis of bone apatite and 80 teeth (21 first premolars, 30 first molars, and 29 s molars) for $\delta^{13}C$ and $\delta^{18}O$ analysis of dental carbonate (Tables 1 and 2). Five first molars, eight first premolars, and seven second molars of the above come from eleven individuals represented by multiple teeth.

### 3.2. Sample selection

The commingled nature of the sample, which included loose teeth as well as teeth in fragmented maxillary and mandibular alveolar bone, necessitated careful sample collection for isotope analysis to prevent individual oversampling. First, the samples were broken down by archaeological context, grouping together teeth or bone most likely coming from an area containing a limited set of individuals. Teeth from

**Table 1**
Isotope results from dental enamel carbonate from the Petra North Ridge.

| ECU Sample # | USF sample # | Context | Database accession # | Tooth | $\delta^{13}C_{ap}$(‰) | $\delta^{18}O$ (‰) VPDB | Age[a] | Sex | DEH count |
|---|---|---|---|---|---|---|---|---|---|
| MEP10 | 33-265 | B.5:32 | B.5:32.h | $LM_1$ | −11.4 | −1.0 | 3 years +/− 12 months | Indeterminate | 0 |
| MEP11 | 33-266 | B.5:32 | B.5:32.g | $RM_1$ | −11.2 | −1.2 | subadult | Indeterminate | 0 |
| MEP16 | 33-271 | B.5:34 | B.5:34.j | $RM^1$ | −11.9 | −1.2 | adult | Indeterminate | 0 |
| MEP17 | 33-272 | B.5:34 mand 11 | B.5:34.k | $LM_1$ | −11.5 | −2.5 | adult | Indeterminate | 0 |
| MEP21 | 33-276 | B.5:35 | B.5:35.n | $RM^1$ | −11.6 | −1.9 | adult | Indeterminate | 0 |
| MEP22 | 33-277 | B.5:35 | B.5:35.r | $RM^1$ | −11.4 | −1.4 | subadult | Indeterminate | 0 |
| MEP23 | 33-278 | B.5:35 | B.5:35.s | $RM^1$ | −11.5 | −2.3 | 3 years +/− 12 months | Indeterminate | 0 |
| MEP25 | 33-279 | B.5:35 | B.5:35.q | $RM_1$ | −12.4 | −0.8 | adult | male | 0 |
| MEP30 | 33-284 | B.6:27 layer 2 #30 | B.6:27.d | $RM_1$ | −11.0 | −1.6 | adult | Indeterminate | 0 |
| MEP32 | 33-286 | B.6:28 | B.6:28.e | $LM^1$ | −11.7 | −1.7 | 3 years +/− 12 months | Indeterminate | 1 |
| MEP33 | 33-287 | B.6:28 | B.6:28.h | $LM^1$ | −11.8 | −2.8 | 4 years +/− 12 months | Indeterminate | 2 |
| MEP34 | 33-288 | B.6:28 | B.6:28.g | RM1 | −11.1 | −1.4 | 4 years +/− 12 months | Indeterminate | 0 |
| MEP36 | 33-289 | B.6:28 | B.6:28.f | RM1 | −12.2 | −2.4 | 7–10 years | Indeterminate | 0 |
| MEP42 | 33-295 | B.6:42 | B.6:42.a | RM1 | −11.8 | −1.3 | adult | Indeterminate | 1 |
| MEP45 | 33297 | B.6:43 | B.6:43.a | RM1 | −11.4 | −1.7 | adult | Indeterminate | 0 |
| MEP49 | 33-300 | B.6:44 | B.6:44.446.b | LM1 | −11.7 | −2.3 | adult | Indeterminate | 0 |
| MEP53 | 33-304 | B.7:20 | B.7:20.h | LM1 | −11.4 | −2.3 | 4 years +/− 12 months | Indeterminate | 0 |
| MEP54 | 33-305 | B.7:20 | B.7:20.g | RM1 | −11.8 | −2.0 | adult | Indeterminate | 0 |
| MEP55 | 33-306 | B.7:25 | B.7:25.a | RM1 | −12.0 | −1.8 | adult | Indeterminate | 0 |
| MEP57 | 33-307 | B.7:25.83 | B.7:25.83.a | RM1 | −10.5 | −1.6 | adult | Indeterminate | 0 |
| MEP59 | 33-309 | B.7:27.76 | B.7:27.76.c | LM1 | −11.4 | −3.1 | adult | Indeterminate | 0 |
| MEP63 | 33-313 | B.7:31 skull E end | B.7:31.l | RM1 | −11.5 | −1.3 | adult | female | 0 |
| MEP66 | 33-316 | B.7:33 with skull 1? | B.7:33.j | LM1 | −11.1 | −3.0 | adult | | 1 |
| MEP69 | 33-319 | B.7:34 mand 3 | B.7:34.a | PM1 | −11.3 | −2.2 | adult | female | 0 |
| MEP70 | 33-320 | B.7:34 mand 3 | B.7:34.e | M1 | −11.7 | −1.9 | adult | female | 0 |
| MEP71 | 33-321 | B.7:34 | B.7:34.g | RM1 | −11.5 | −1.4 | 3 years +/− 12 months | Indeterminate | 0 |
| MEP74 | 33-324 | F.1:26.120 | F.1:26.120.16.a | LM1 | −11.4 | −1.4 | adult | Indeterminate | 0 |
| MEP78 | 33-328 | F.1:28.97 | F.1:28.97.69.a | LM1 | −11.3 | −1.3 | adult | Indeterminate | 0 |
| MEP80 | 33-330 | F.1:28.102 | F.1:28.102.S40.s | RM1 | −11.7 | −2.9 | adult | Indeterminate | 0 |
| MEP82 | 33-332 | F.1:28.115 | F.1:28.115.35.f | RM1 | −12.3 | −0.9 | adult | Indeterminate | 0 |
| MEP87 | 33-337 | F.1:30.134 individual 3 | F.1:30.134.S20.s | RM1 | −11.6 | −0.9 | subadult | Indeterminate | 0 |
| MEP02 | 33-259 | B.4:23 | B.4:23a | RPM1 | −11.6 | −1.5 | adult | Indeterminate | 0 |
| MEP12 | 33-267 | B.5:34 skull 13 | B.5:34.55.a | RPM1 | −10.9 | −2.4 | adult | Indeterminate | 3 |
| MEP13 | 33-268 | B.5:34 max 20 | B.5:34.53.d | RPM1 | −11.1 | −1.8 | adult | Indeterminate | 0 |
| MEP14 | 33-269 | B.5:34 from mand 20 | B.5:34.b | RPM1 | −11.2 | −1.9 | adult | Indeterminate | 1 |
| MEP15 | 33-270 | B.5:34 | B.5:34.47.a | RPM1 | −11.1 | −2 | adult | Indeterminate | 0 |
| MEP20 | 33-275 | B.5:35 | B.5:35.b | RPM1 | −11.4 | −1.3 | adult | Indeterminate | 1 |
| MEP28 | 33-282 | B.6:6 layer 6 | B.6:6.c | RPM1 | −11.5 | −1.5 | adult | Indeterminate | 0 |
| MEP29 | 33-283 | B.6:27 layer 2 #30 | B.6:27.b | LPM1 | −10.9 | −1.6 | adult | Indeterminate | 0 |
| MEP41 | 33-294 | B.6:42 | B.6:42.418.a | LPM1 | −11.2 | −2.3 | adult | Indeterminate | 0 |
| MEP48 | 33-299 | B.6:44 | B.6:44.447.a | LPM1 | −10.5 | −2.5 | adult | Indeterminate | 1 |
| MEP52 | 33-303 | B.7:20 | B.7:20.488.c | LPM1 | −11.4 | −3.8 | adult | Indeterminate | 1 |
| MEP58 | 33-308 | B.7:27 | B.7:27.a | RPM1 | −11.2 | −3.0 | adult | Indeterminate | 0 |
| MEP61 | 33-311 | B.7:31 cranium E end | B.7:31.a | RPM1 | −11.4 | −2.1 | adult | female | 1 |
| MEP62 | 33-312 | B.7:31 cranium/mandible W end | B.7:31.c | LPM1 | −10.6 | −3.3 | adult | male | 0 |
| MEP68 | 33-318 | B.7:34 mandible 3? | B.7:34.b | LPM1 | −11.3 | −2.3 | adult | female | 0 |
| MEP73 | 33-323 | B.7:35 | B.7:35.a | LPM1 | −11.0 | −3.2 | adult | Indeterminate | 1 |
| MEP76 | 33-326 | F.1:28.90 | F.1:28.90.S1.bo | LPM1 | −11.1 | −2.4 | adult | Indeterminate | 2 |
| MEP81 | 33-331 | F.1:28.115 | F.1:28.115.S34.aa | RPM1 | −11.6 | −0.5 | adult | Indeterminate | 0 |
| MEP84 | 33-334 | F.1:28.115 | F.1:28.115.35.n | RPM1 | −12.0 | −0.9 | adult | Indeterminate | 0 |
| MEP85 | 33-335 | F.1:28.141 | F.1:28.141.14 | RPM1 | −11.3 | −3.1 | adult | Indeterminate | 0 |
| MEP01 | 33-258 | B.4:10 | B.4:10.a | RM2 | −11.1 | −1.7 | adult | Indeterminate | 0 |
| MEP04 | 33-260 | B.4:23 “teeth bag” | B.4:23.c | LM2 | −11.3 | −2.4 | adult | Indeterminate | 0 |
| MEP05 | 33-261 | B.4:23 “teeth bag” | B.4:23.d | LM2 | −11.6 | −2.4 | adult | Indeterminate | 0 |
| MEP06 | 33-262 | B.4:23 individual 2 | B.4:23.e | RM2 | −11.4 | −1.9 | adult | Indeterminate | 0 |
| MEP07 | 33-263 | B.5:11 | B.5:11.a | LM2 | −12.5 | −2.4 | adult | Indeterminate | 0 |
| MEP09 | 33-264 | B.5:31 | B.5:31.a | LM2 | −13.3 | −4.7 | adult | male | 0 |
| MEP18 | 33-273 | B.5:34 max 20 | B.5:34.53.a | LM2 | −11.3 | −2.0 | adult | Indeterminate | 1 |
| MEP19 | 33-274 | B.5:34 | B.5:34.l | M2 | −11.4 | 1.1 | adult | Indeterminate | 0 |
| MEP26 | 33-280 | B.5:35 skull 13 | B.5:35.55.a | LM2 | −11.1 | −2.2 | adult | Indeterminate | 0 |
| MEP27 | 33-281 | B.5:35 skull(?) 27 | B.5:35.a | RM2 | −11.3 | −2.3 | adult | Indeterminate | 0 |
| MEP31 | 33-285 | B.6:27 layer 2 #30 | B.6:27.30.a | RM2 | −12.0 | −1.7 | adult | Indeterminate | 0 |
| MEP37 | 33-290 | B.6:28 | B.6:28.250.c | RM2 | −11.7 | −2.9 | adult | Indeterminate | 0 |
| MEP38 | 33-291 | B.6:31.110 | B.6:31.343.110.c | RM2 | −10.5 | −3.1 | adult | Indeterminate | 0 |
| MEP39 | 33-292 | B.6:34 | B.6:34.c | LM2 | −11.2 | −1.7 | adult | Indeterminate | 0 |

(*continued on next page*)

**Table 1** (*continued*)

| ECU Sample # | USF sample # | Context | Database accession # | Tooth | $\delta^{13}C_{ap}$(‰) | $\delta^{18}O$ (‰) VPDB | Age[a] | Sex | DEH count |
|---|---|---|---|---|---|---|---|---|---|
| MEP40 | 33-293 | B.6:39 | B.6:39.a | LM2 | −12.1 | −1.6 | adult | Indeterminate | 0 |
| MEP43 | 33-296 | B.6:42 | B.6:42.418.b | LM2 | −11.1 | −2.6 | adult | Indeterminate | 0 |
| MEP46 | 33-298 | B.6:43 | B.6:43.435.c | LM2 | −11.9 | −1.1 | adult | Indeterminate | 1 |
| MEP50 | 33-301 | B.6:44 | B.6:44.446.a | LM2 | −11.9 | −1.5 | adult | Indeterminate | 0 |
| MEP51 | 33-302 | B.6:44 | B.6:44.a | LM2 | −11.2 | −1.7 | adult | Indeterminate | 0 |
| MEP60 | 33-310 | B.7:27.76 | B.7:27.76.a | RM2 | −11.3 | −3.3 | adult | Indeterminate | 1 |
| MEP64 | 33-314 | B.7:31 | B.7:31.b | LM2 | −10.8 | −3.2 | adult | Indeterminate | 0 |
| MEP65 | 33-315 | B.7:31 skull W end | B.7:31.m | RM2 | −11.0 | −3.1 | adult | male | 0 |
| MEP67 | 33-317 | B.7:33 | B.7:33.499.a | RM2 | −10.5 | −1.9 | adult | Indeterminate | 1 |
| MEP72 | 33-322 | B.7:34 “crania” | B.7:34.533.a | RM2 | −6.6 | 1.0 | adult | Indeterminate | 0 |
| MEP75 | 33-325 | F.1:27.123 | F.1:27.123.S1.bb | RM2 | −12.1 | 0.3 | adult | Indeterminate | 0 |
| MEP77 | 33-327 | F.1:28.94 | F.1:28.94.S1.ai | LM2 | −11.1 | −2.5 | adult | Indeterminate | 0 |
| MEP79 | 33-329 | F.1:28.97 | F.1:28.97.69.a | LM2 | −11.4 | −3.0 | adult | Indeterminate | 0 |
| MEP83 | 33-333 | F.1:28.115 | F.1:28.115.35.f | RM2 | −11.5 | −0.4 | adult | Indeterminate | 0 |
| MEP86 | 33-336 | F.1:30.139 | F.1:30.139.S1 | LM2 | −11.7 | 0.2 | 8–9 years | Indeterminate | 0 |

[a] Age estimates of subadults was based on dental formation stage using Moorrees et al. (1963) and Šešelj et al. (2019). Completely formed M1s were classified as “subadult” if they had an attrition wear stage or 1 or 2 based on Buikstra and Ubelaker (1994). Completely formed M1s with a wear stage of at least 3 and completely formed PM1s and M2s were classified as “adult”

each tooth class and each element were observed for position (left or right, upper or lower), level of wear, taphonomic changes, and size to ensure only one of each tooth type or bone was selected from a subset of remains likely coming from the same individual. If possible, selection was limited to certain teeth or bones from a particular context (e.g., all left lower first molars). Certain teeth were prioritized in sample collection, including those associated with other teeth in the same piece of alveolar bone, or those which had already been processed for other isotope analyses ($^{87}Sr/^{86}Sr$).

### 3.3. Methods

#### 3.3.1. Enamel hypoplastic defects

Dental enamel hypoplastic defects were observed in the anterior dentition (incisors and canines) using a 10X hand-held loupe and distance from the center of each defect to the cemento-enamel junction (CEJ) measured using a pair of standard digital sliding calipers. Age of defect occurrence in this sample with notable dental attrition relied on a traditional linear regression approach by Goodman and Rose (1990). The results were interpreted considering the degree of occlusal wear in the sample in addition to issues with age of occurrence estimation.

#### 3.3.2. Age and sex estimation

The commingled nature of the assemblage hindered attributing age and sex to many of the samples. Dental eruption stage provided age estimates for some subadult dental enamel samples using Moorrees et al. (1963) and Šešelj et al. (2019). For comparison of isotope values by life stage, an incomplete or completely formed M1 with an occlusal wear stage of 1 or 2 based on Buikstra and Ubelaker (1994) was classified as “subadult”. Dental enamel samples belonging to “adults” were identified by completion of PM1 or M2 root formation or a completely formed M1 with an occlusal wear stage of at least 3. In most cases, bone samples were simply classified as “adult” if they had fused epiphyses or other indicators of complete formation, and in cases where they could be linked to a pelvis, pubic symphyseal and auricular surface degeneration provided a more accurate age estimate (Brooks and Suchey, 1990; Lovejoy et al., 1985). The dental and bone samples only were assigned a sex estimate if they were associated with a skull or mandible with observable morphological sexually-dimorphic features following Buikstra and Ubelaker (1994). Samples that could be linked to linked to an os coxa utilized a morphological sex estimation following Phenice (1969). Metric techniques based on Mediterranean samples were used to estimate the sex of complete metacarpals (Manolis et al., 2009) and metatarsals (Mountrakis et al., 2010). Other long bone and incomplete metacarpal metrics based on North American populations (Spradley and Jantz, 2011; Stojanowski, 1999) were used for sex estimation if necessary.

#### 3.3.3. Dental enamel

The processing of the dental enamel samples for stable isotope analysis occurred in the Laboratory for Archaeological Science & Technology (LAST) at the University of South Florida in Tampa, Florida (Tykot, 2018). The teeth selected for isotope analysis were cleaned using a brush and distilled water. After drying, a drill was used to remove the enamel surface and at least 10 mg of enamel powder was extracted from internal enamel. Powdering of larger pieces using a porcelain mortar and pestle was completed if necessary. The enamel powder of all samples was weighed and placed in 2% sodium hypochlorite for 24 h. The samples were then centrifuged after which the sodium hypochlorite solution was poured off and replaced with distilled water four times. This was followed by at least 24 h in the drying oven. After being weighed again, the samples underwent 24 h in 1.0 M buffered acetic acid. The same centrifuging and pouring off process as before was implemented followed by at least 24 h in the drying oven and a third round of weighing the remaining sample. The last step was to remove ~ 1 mg of the sample and place it in a separate vial for stable isotope analysis. Any powdered enamel left over was stored in case one of the samples needed to be run again and/or for future isotopic analyses.

Once all samples were prepared, they were run on a ThermoFisher MAT253 isotope ratio mass spectrometer coupled to a GasBench-II + continuous-flow interface in the Paleolab at the University of South Florida. The solid samples were first reacted with 600 µl of 104% phosphoric acid ($H_3PO_4$) at 25° C for 24 h. Both carbon and oxygen stable isotope data are reported relative to the Vienna PeeDee Belemnite (V-PDB) standard. The precision of stable isotope ratio mass spectrometry analysis is ± 0.1‰ for both $\delta^{13}C$ and $\delta^{18}O$.

#### 3.3.4. Bone apatite

The human bone samples were prepared by removing the outer layer of cortical bone and any internal trabecular bone using a Dremel drill to reduce diagenetic and environmental contaminants (Slovak et al., 2009). The samples were subsequently crushed in a porcelain mortar using a pestle and 30 mg of the < 250 µm fraction was prepared for apatite analysis following a modified Nielsen-Marsh and Hedges method (2000) that involved treatment with 1.0 M normal acetic acid. Samples were left overnight then rinsed three times with distilled water and dried overnight at 50° C. The $\delta^{13}C$ and $\delta^{18}O$ of

**Table 2**
Isotope results and FTIR-ATR parameters from bone apatite from the Petra North Ridge Project and FTIR-ATR results of modern animal bone controls.

| ECU Sample # | U of A sample # | Context | Database accession # | Element | $\delta^{13}C_{ap}$ (‰) | Age | Sex | CI (1σ) | C/P (1σ) |
|---|---|---|---|---|---|---|---|---|---|
| PAP1 | PAP-01/PERRY/K788 | B.5:31 | no acc # | long bone frag | −13.7 | Adult | Female | 4.89 (0.35) | 0.14 (0.01) |
| PAP2 | PAP-02/PERRY/K788 | B.5:17 | B.5:17.CN1-CN7 | humerus | −12.7 | 18–20 years | Female | 4.90 (0.42) | 0.12 (0.03) |
| PAP3 | PAP-03/PERRY/K788 | B.5:9 individual 1 | B.5:9.CN401 | ribs | −13.1 | Adult | Female | 4.80 (0.35) | 0.10 (0.00) |
| PAP4 | PAP-04/PERRY/K788 | B.5:12 | no acc # | ribs | −13.7 | Adult | Male | 4.13 (0.53) | 0.26 (0.02) |
| PAP5 | PAP-05/PERRY/K788 | B.4:18 | B.4:18.CN1? (MC3) | MT3 | −13.6 | Adult | Indeterminate | 5.00 (0.00) | 0.27 (0.00) |
| PAP6 | PAP-06/PERRY/K788 | B.4.17 | B.4:17.CN1 | MT4 | −13.1 | Adult | Male | 4.80 (0.35) | 0.13 (0.02) |
| PAP7 | PAP-07/PERRY/K788 | B.4:22 | B.4:22.CN1 | MC3 | −13.5 | Adult | Male | 3.88 (0.18) | 0.41 (0.03) |
| PAP8 | PAP-08/PERRY/K788 | B.4:23 individual 1 | B.4:23.CN201/INDIV-2 | MT3 | −12.5 | Adult | Male | 4.18 (0.02) | 0.29 (0.02) |
| PAP9 | PAP-09/PERRY/K788 | B.4:23 individual 2 | B.4:23.CN1/INDIV-2 | MT3 | −13.0 | Adult | Male | 3.38 (0.21) | 0.27 (0.03) |
| PAP10 | PAP-10/PERRY/K788 | B.4:23 individual 3 | B.4:23.CN1/INDIV-3 | MC5 | −13.2 | Adult | Indeterminate | 4.83 (0.47) | 0.14 (0.01) |
| PAP12 | PAP-12/PERRY/K788 | B.4:10 individual 1 | B.4:10.CN1 | humerus | −12.8 | Adult | Indeterminate | 4.86 (0.20) | 0.14 (0.00) |
| PAP13 | PAP-13/PERRY/K788 | B.4:10 individual 2 | B.4:10.CN2 | humerus | −13.6 | Adult | Female | 4.80 (0.57) | 0.18 (0.00) |
| PAP14 | PAP-14/PERRY/K788 | B.4:10 individual 3 | B.4:10.CN3 | humerus | −13.3 | Adult | Indeterminate | 4.59 (0.24) | 0.18 (0.04) |
| PAP15 | PAP-15/PERRY/K788 | B.5:15 skull #1 | B.5:15.CNa1/SKULL-1 | cranial frag | −13.5 | old adult | Poss female | 5.18 (0.17) | 0.10 (0.01) |
| PAP16 | PAP-16/PERRY/K788 | B.5:15 skull #2 | no acc # | parietal | −13.6 | Adult | Male | 4.92 (0.12) | 0.12 (0.01) |
| PAP17 | PAP-17/PERRY/K788 | B.5:15 skull #4 | B.5:15.CNc1/SKULL4 + | parietal | −13.2 | Adult | Male | 4.74 (0.25) | 0.16 (0.03) |
| PAP18 | PAP-18/PERRY/K788 | B.5:15 skull #5 | B.5:15.CNd1/SKULL-5 | cranial frag | −14.0 | Adult | Female possible | 4.75 (0.35) | 0.14 (0.03) |
| PAP19 | PAP-19/PERRY/K788 | B.5:15 skull #6 | B.5:15/CNe1/SKULL-6 | cranial frag | −13.4 | Adult | Male | 4.70 (0.43) | 0.13 (0.02) |
| PAP20 | PAP-20/PERRY/K788 | B.5:15 skull #7 | B.5:15.CNf1/SKULL-7 | cranial frag | −12.7 | Adult | Female | 4.86 (–) | 0.13 (–) |
| PAP21 | PAP-21/PERRY/K788 | B.5:15 skull #9 | B.5:15.CNh1/SKULL-9 | parietal | −13.1 | Adult | Female possible | 4.68 (0.07) | 0.16 (0.00) |
| PAP22 | PAP-22/PERRY/K788 | B.5:15 skull #10 | B.5:15/CNj1/SKULL-10 | cranial frag | −12.9 | Adult | Male possible | 4.86 (0.00) | 0.14 (0.00) |
| PAP23 | PAP-23/PERRY/K788 | B.5:9 skull #11 | B.5:9.CN301-CN309/SKULL#11 | parietal | −13.7 | Adult | Male | 4.29 (0.77) | 0.16 (0.04) |
| PAP24 | PAP-24/PERRY/K788 | B.5:15 skeleton #1 | no acc # | ribs | −13.2 | Adult | Male | 4.64 (0.51) | 0.14 (0.00) |
| PAP25 | PAP-25/PERRY/K788 | Tomb 2 burial 1 | no acc # | femur | −13.2 | 20–24 | Female | 4.61 (0.14) | 0.19 (0.02) |
| PAP26 | PAP-26/PERRY/K788 | Tomb 2 burial 2 | no acc # | long bone frag | −10.8 | 45–49 | Indeterminate | 3.67 (0.47) | 0.35 (0.02) |
| PAP27 | PAP-27/PERRY/K788 | Tomb 2 burial 4 | no acc # | femur | −11.1 | 25–29 | Male | 4.60 (0.37) | 0.16 (0.02) |
| PAP28 | PAP-28/PERRY/K788 | Tomb 2 burial 5 | no acc # | femur | −11.1 | 50–59 | Female | 4.50 (0.14) | 0.20 (0.01) |
| PAP29 | PAP-29/PERRY/K788 | Tomb 2 burial 6 | no acc # | femur | −10.4 | 35–39 | Female | 4.50 (0 3 0) | 0.17 (0.00) |
| PAP30 | PAP-30/PERRY/K788 | Tomb 2 burial 8 | no acc # | femur | −12.7 | 18–20 | Female | 4.17 (0.24) | 0.29 (0.00) |
| MA3 | | | | *Modern deer* | | | | 2.98 (0.32) | 0.52 (0.02 |
| MA4 | | | | *Modern deer* | | | | 3.13 (0.53) | 0.52 (0.02) |
| MA5 | | | | *Modern deer* | | | | 3.61 (0.35) | 0.32 (0.06) |
| MA9 | | | | *Modern deer* | | | | 3.06 (0.34) | 0.51 (0.02) |
| MA10 | | | | *Modern deer* | | | | 2.98 (0.32) | 0.52 (0.02) |
| MA11 | | | | *Modern deer* | | | | 2.65 (0.21) | 0.47 (0.04) |

carbonates were measured at the Environmental Isotope Laboratory at the Department of Geosciences at the University of Arizona using an automated carbonate preparation device (KIEL-III) coupled to a gas ratio mass spectrometer (Finnigan MAT 252). Powdered samples were reacted with dehydrated phosphoric acid under vacuum at 70° C. The isotope ratio measurement is calibrated based on repeated measurements of NBS-19 and NBS-18 and precision is ± 0.11‰ for $\delta^{18}O$ and ± 0.08‰ for $\delta^{13}C$ (1 σ). The results are reported relative to the V-PDB standard.

### 3.3.5. Identifying diagenetic change

The poor collagen preservation of the human bone samples from Petra necessitated checking the level of diagenetic changes in bone apatite using Fourier transform infrared spectral analysis using attenuated total reflection (FTIR-ATR). This relatively new method for analyzing archaeological bone tissues provides data similar to FTIR-KBr but can utilize solid bone or bone powder and does not require removing part of the sample to create KBr pellets (Beasley et al., 2014; dal Sasso et al., 2016; Hollund et al., 2013; Lebon et al., 2016; Stathopoulou et al., 2008; Thompson et al., 2009). Untreated ground bone samples were sieved through a 250 μm mesh and placed directly on the diamond surface of a ThermoFisher Nicolet iS50 FTIR spectrometer at East Carolina University Department of Chemistry's GMS Laboratory with the experimental setup of 32 scans at a spectral resolution of 8 $cm^{-1}$ and a wavenumber range of 4000–400 $cm^{-1}$. Each spectrum was corrected for depth of penetration and baseline correction was performed manually. The crystallinity index (CI) or infrared splitting factor (IR-SF) was calculated following Weiner and Bar-Yosef (1990) and carbonate to phosphate ratios were computed based on the phosphate peak height at 1030 $cm^{-1}$ and the carbonate peak height at 1415 $cm^{-1}$ in the wavelength spectrum (Wright and Schwarcz, 1996). To control for possible heterogeneity of the bone powder samples, spectrum capture was repeated 2 or 3 times after manipulating the powder on the prism. Values for each sample are reported as means ± 1σ excepting one sample with a single spectrum (PAP20). Ground bone samples from six modern deer were also run as controls to assess the ancient bone preservation.

### 3.3.6. Statistical comparisons

The isotope values of each tooth class were tested for significant differences using Kruskal-Wallace test followed by Dunn test, and differences in intra-tooth class variation explored using a Levene's test. In addition, comparisons of mean isotope values between adults and subadults were accomplished using a Mann-Whitney *U* test and variation using a Levene's test. Finally, differences between tombs was explored using a Kruskal-Wallace followed by a Dunn test, and differences in variation utilized a Levene's test. Tomb identification of samples from B.4, B.5, B.6, B.7, or F.1 is noted in the first number and letter of the context information of a sample.

## 4. Results

### 4.1. Carbon isotopes

Isotopic results of adult bone apatite from the Petra North Ridge tombs reflect a general reliance on $C_3$ sources, although some individuals show significant $C_4$ contributions ($\delta^{13}C_{apatite}$ $\bar{X}$ = −12.9‰ ± 0.9) (Table 1; Fig. 2). The overall dental enamel $\delta^{13}C$ values range between −13.3‰ and −6.6‰ ($\bar{X}$ = −11.4 ± 0.7‰), slightly less negative than the adult bone apatite $\delta^{13}C$ values. The $\delta^{13}C$ for the youngest-forming teeth, the first molars, averages −11.6‰ (± 0.4‰). Values increase slightly in the next teeth to develop, the premolars ($\bar{X}$ = −11.2 ± 0.3‰) and stay essentially the same through the development of the second molars ($\bar{X}$ = −11.3 ± 1.1‰). Only the difference between the first molars and the other two teeth was found to be significant (Table 3). A Levene's test found differences in variances across the tooth classes and tissues (F ratio = 2.9445; p = 0.0364), with the M2 and human bone values having larger standard deviations that the M1 or PM1.

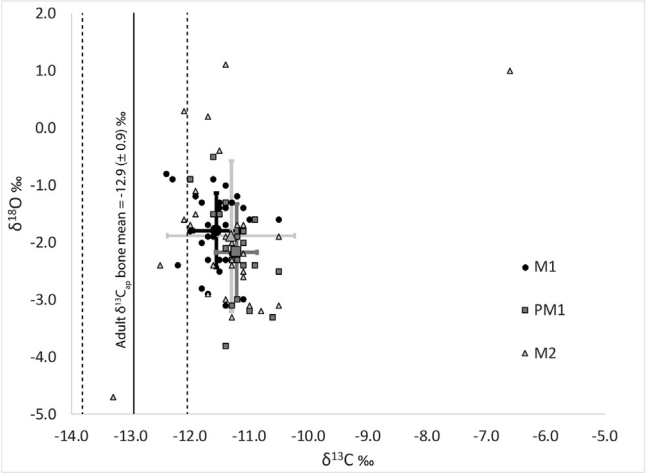


**Fig. 2.** Plot of the $\delta^{13}C$ and $\delta^{18}O$ values by tooth type in the Petra North Ridge sample, including means and standard deviations.

The eleven individuals for whom we have multiple teeth demonstrate notable heterogeneity in the direction and magnitude of $\delta^{13}C$ shifts with age (Fig. 3). The means of this subsample (M1 $\bar{X}$ = −11.6 ± 0.4‰; PM1 $\bar{X}$ = −11.1 ± 0.3‰; M2 $\bar{X}$ = −11.4 ± 0.4‰) generally follow the pattern of the overall sample. However, the larger standard deviation in the M2 seen in the complete sample is not reflected here. The three individuals for whom we have both an M1 and a PM1 do mirror the increase seen in the overall sample, although to varied degrees. However, the shift between PM1 and M2 varies between individuals, with one showing a large decrease (B.6:27 layer #2 #30), some a slight decrease, and in one case, B.6:42.418, an increase with age. In addition, $\delta^{13}C$ in the first molar is higher than the second molar in two individuals, and in three cases it is lower. Although as noted above the bone apatite values representing the adults may not be directly comparable to the dental enamel values here, the $\delta^{13}C$ values after development of the PM1 generally trends downwards toward the values representing the adult diet.

### 4.2. Oxygen isotopes

The $\delta^{18}O$ of all teeth tested ranges between −4.7‰ and +1.1‰ ($\bar{X}$ = −1.9 ± 1.0‰). This standard deviation is comparable to that seen within other archaeological sites in the region (Gregoricka and Sheridan, 2017; Perry et al., 2009). The first molar $\delta^{18}O$ values average −1.8 (± 0.7‰), and the values decline only slightly with the first molars ($\bar{X}$ = −2.2 ± 0.8‰) before slightly increasing again in the second molars ($\bar{X}$ = −1.9 ± 1.3‰). None of these shifts were found to be statistically significant (Table 3), and thus the expected decrease in $\delta^{18}O$ with the shift from breastfeeding to relying on environmental water was not identified. A Levene's test found that the M2 had significantly more variation within this sample than the M1 (F ratio = 5.8708, p = 0.0185).

Analysis of the $\delta^{18}O$ shifts by individual clearly shows that the stasis across tooth classes seen in the entire sample actually masks intra-sample variation, although the means for this subset are not different from the complete sample (M1 $\bar{X}$ = −1.6 ± 0.5‰; PM1 $\bar{X}$ = −2.3 ± 0.5‰; M2 $\bar{X}$ = −2.2 ± 0.9‰) (Fig. 4) except for a statistically significant decline from the M1 to the PM1 (Z = −2.2513; p = 0.0244). Similar to the complete sample, the M2 shows the greatest standard deviation. Two individuals have the expected decrease from

**Table 3**
Comparisons of mean isotope data across tooth classes.

| Isotope | Tooth | N | Mean (sd) ‰ | Kruskal-Wallace Results | Dunn Test Results |
|---|---|---|---|---|---|
| $\delta^{13}C$ | M1 | 21 | –11.6 (0.4) | **$X^2$ = 6.8569, p = 0.0324** | **M1 vs. PM1 Z = 2.59071, p = 0.0287** |
| | PM1 | 30 | −11.2 (0.3) | | PM1 vs. M2 Z = -1.23747, p = 0.6477 |
| | M2 | 29 | −11.3 (1.1) | | M1 vs. M2 Z = -1.46322, p = 0.4302 |
| $\delta^{18}O$ | M1 | 21 | −1.8 (0.7) | $X^2$ = 2.5847, p = 0.2746 | M1 vs. PM1 Z=–1.44531, p = 0.4451 |
| | PM1 | 30 | −2.3 (0.5) | | PM1 vs. M2 Z = 0.28046, p = 1.000 |
| | M2 | 29 | −2.2 (0.9) | | M1 vs. M2 Z = -1.26481, p = 0.6178 |

M1 to PM1 and two from PM1 to M2. In addition, two individuals with only an M1 and M2 show the decline, with the unavailable PM1 value presumably falling in between. However, four individuals show an increase in $\delta^{18}O$ with age, either from the M1 to M2 or the PM1 to M2. The one individual with all three teeth (B.6:27layer #2 #30) has little to no change across tooth classes.

### 4.3. FTIR-ATR analysis of bone apatite

The CI and C/P of the Petra samples demonstrate the expected linear relationship between the two variables, for greater diagenetic alteration results in increased crystal length indicated by the CI that trends with increased carbonate loss identified by a decrease in the C/P ratio (Sillen, 1989) (Fig. 5). The modern animal bone has CI values ranging between 2.65 and 3.61 and C/P ratios from 0.32 to 0.52. The archaeological human bone indicates for the most part greater diagenetic alteration of apatite than the modern samples, with CI values between 3.38 and 5.18 and C/P values from 0.10 to 0.41. The $\delta^{13}C$ values did not pattern with either parameter, suggesting that while diagenetic alteration has occurred with some samples, it has not resulted in major outliers in $\delta^{13}C$.

### 4.4. Inter-tomb comparisons

Comparison of $\delta^{13}C$ and $\delta^{18}O$ results by tomb meant to identify possible lineal-related differences in childhood diet. Tomb identification for each sample is noted by the letter and first number in the context column in Table 1 (i.e., B.4, B.5, B.6, B.7, and F.1). Similar to the entire sample, the heterogeneity of samples by tomb increases with age (i.e., from the M1 to the PM1 to the M2 (Table 4). However, some notable patterns emerge in terms of consistent differences across tooth classes by tomb, particularly the divergence of tomb B.7 from the other tombs in the PM1 oxygen value and the M2 carbon value, including its large standard deviation in the latter. Tomb F.1 also has higher diversity in oxygen isotope values in all tooth classes than the other tombs, and the heterogeneity seen in the M2 oxygen values in B.5, B.7, and F.1 are not shared by B.4 and B.6.

### 4.5. Isotopes and childhood mortality

Possible dietary differences in infancy, represented by $\delta^{13}C$ of the M1 enamel, between individuals that did or did not survive childhood found that the sample means were essentially equal (adult survivors $\bar{X}$ = −11.5 ± 0.4‰; deceased children $\bar{X}$ = −11.5 ± 0.3‰; Z = 0.26002, p = 0.7948), although the adult survivors had slightly greater variability than the deceased children (F ratio = 1.1855, p = 0.2855). The mean $\delta^{18}O$ values of the M1 between adult survivors and deceased children did not differ in their sample means (adult survivors $\bar{X}$ = −1.9 ± 0.7‰; deceased children $\bar{X}$ = −1.7 ± 0.6‰; Z = −0.5842, p = 0.5603) or standard deviations (F = 0.0107, p = 0.9183).

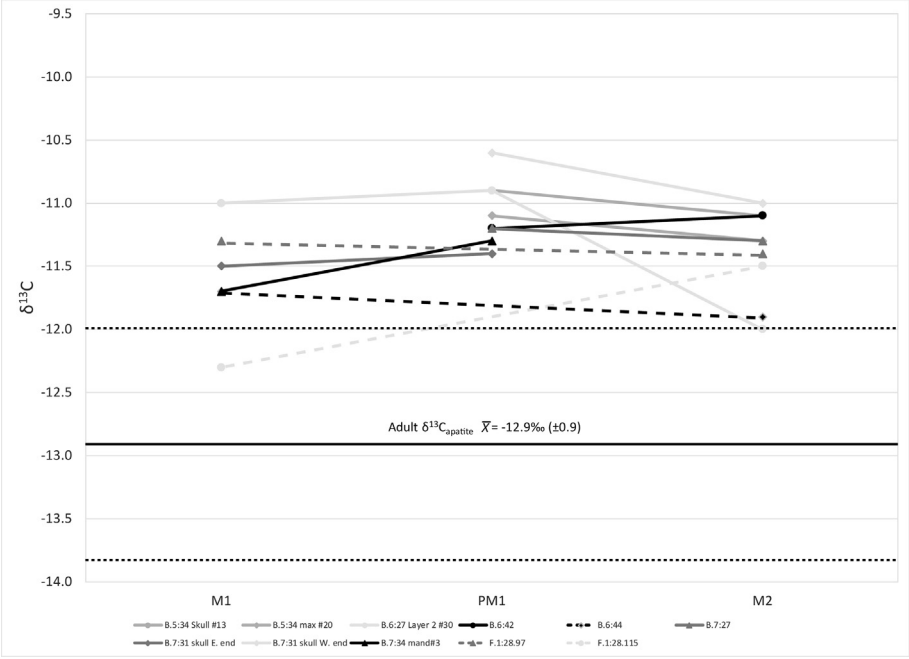


**Fig. 3.** $\delta^{13}C$ values across tooth classes for the 11 individuals with multiple teeth. Dashed lines connect linked M1 and M2 values for individuals without available PM1s.

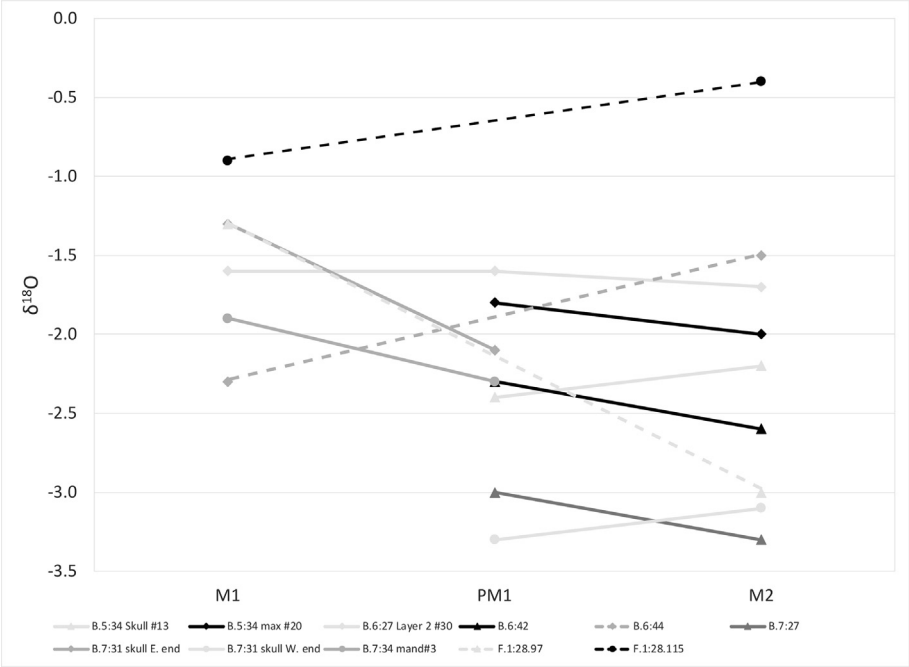


**Fig. 4.** $\delta^{18}O$ values across tooth classes for the 11 individuals with multiple teeth. Dashed lines connect linked M1 and M2 values for individuals without available PM1s.

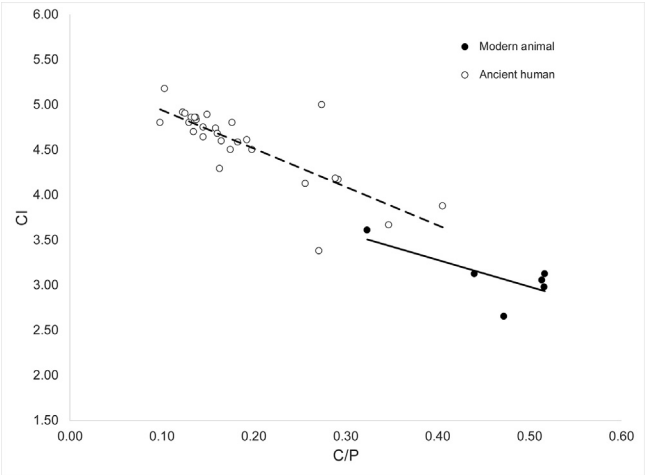


**Fig. 5.** Plot of CI and C/P values for modern deer and archaeological human bone samples from Petra.

**Table 4**
$\delta^{13}C$ and $\delta^{18}O$ means and standard deviations of tooth classes in the Petra North Ridge sample by Tomb I.D.

| Tooth class | Tomb I.D. | N | $\delta^{13}C$ ‰ | $\delta^{18}O$ ‰ |
|---|---|---|---|---|
| M1 | B.4 | 0 | – | – |
| | B.5 | 8 | −11.6 ± 0.4 | −1.5 ± 0.6 |
| | B.6 | 8 | −11.6 ± 0.4 | −1.9 ± 0.5 |
| | B.7 | 10 | −11.4 ± 0.4 | −2.1 ± 0.6 |
| | F.1 | 5 | −11.6 ± 0.4 | −1.5 ± 0.8 |
| | All tombs | 30 | −11.6 ± 0.4 | −1.8 ± 0.7 |
| PM1 | B.4 | 1 | −11.6 | −1.5 |
| | B.5 | 5 | −11.1 ± 0.2 | −1.9 ± 0.4 |
| | B.6 | 4 | −11.0 ± 0.4 | −2.0 ± 0.5 |
| | B.7 | 6 | −11.2 ± 0.3 | −3.0 ± 0.6 |
| | F.1 | 4 | −11.5 ± 0.4 | −1.7 ± 1.2 |
| | All tombs | 21 | −11.2 ± 0.3 | −2.2 ± 0.8 |
| M2 | B.4 | 4 | −11.4 ± 0.2 | −2.1 ± 0.4 |
| | B.5 | 6 | −11.8 ± 0.9 | −2.1 ± 1.9 |
| | B.6 | 9 | −11.5 ± 0.5 | −2.0 ± 0.7 |
| | B.7 | 5 | −10.0 ± 1.9 | −2.1 ± 1.8 |
| | F.1 | 5 | −11.5 ± 0.4 | −1.8 ± 1.6 |
| | All tombs | 29 | −11.3 ± 1.1 | −1.9 ± 1.3 |

### *4.6. Age of enamel hypoplastic defect formation*

Out of 405 incisors and canines in the PNRP sample, 44, or 11% displayed at least one hypoplastic defect. The frequency of defect formation in these teeth begins increasing around 2 years of age, with a mean age of occurrence of 3.7 years (Fig. 6).

## 5. Discussion

### *5.1. Variability in $C_3$ versus $C_4$ consumption in Petra children*

This isotopic study of childhood diet using $\delta^{13}C$ and $\delta^{18}O$ in enamel carbonate demonstrated that individuals at Petra seemingly followed no strong cultural dictates regarding the composition of childhood diet or water-altering behaviors, and perhaps, the timing of weaning. The bulk samples utilized here, which not only combine the dietary inputs across years of dental enamel formation, but also overlap in developmental timing, do not allow identification of clear shifts in diet and breastfeeding. In general, the $\delta^{13}C$ values of all tooth classes are less negative than the adult bone values suggesting they consumed more $C_4$ sources than adults, although isotopes in these two tissues may not reflect diet or physiology in the same manner. Assessing the overall sample would suggest this difference reflects a small ~ 1‰ mother-infant effect between that may be seen in $\delta^{13}C$ (DeNiro and Epstein, 1978; Fuller et al., 2006). Parsing the shifts between tooth classes by individual and even by tomb demonstrates heterogeneity in childhood diet in this community, and thus factors other than mother-infant offsets or strict diets are affecting isotopic shifts. The diet in early infancy replicated in the M1, reflecting a combination of the maternal diet during breastfeeding as well as possible solid food introduction during weaning, shows a varied proportion of $C_4$ foods over the period of enamel formation. While the stronger $C_4$ signature in infant than adult diets could indicate that breastfeeding mothers consumed more $C_4$

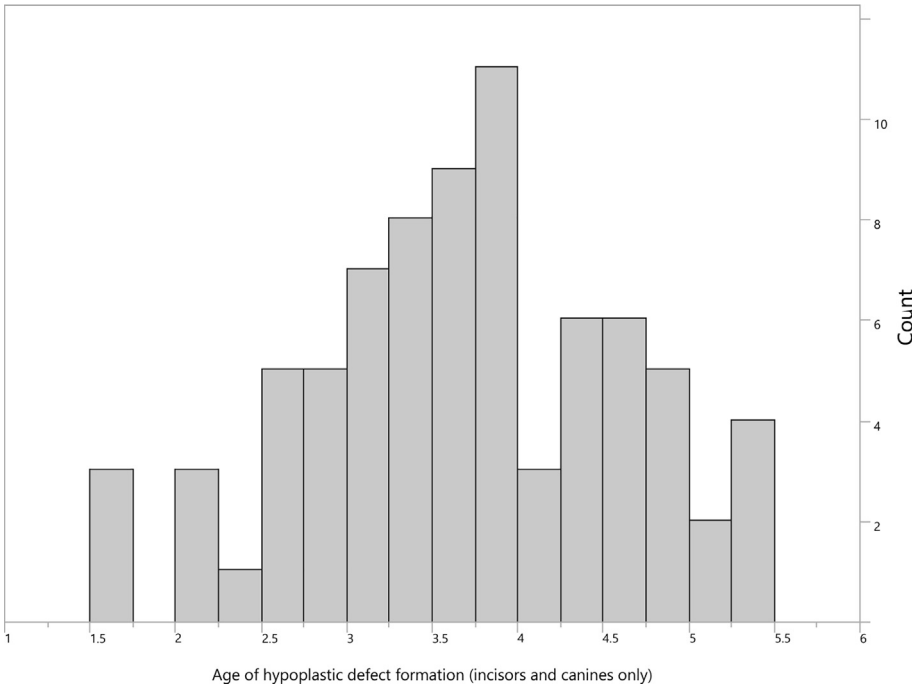


**Fig. 6.** Age of LEH occurrence within the Petra North Ridge sample.

foods on average than other adults, this also can reflect varied proportions of $C_3$ versus $C_4$ solid foods in the infant diet or when $C_4$-based solid foods supplemented breastmilk having a $C_3$ signature. In some children, the proportion of $C_4$ foods, either in relation to consumption of $C_3$ resources in solid food or breastmilk from $C_3$ consumers, increases with age based on the less negative values in PM1 enamel. The consumption of more $C_4$ foods than adults continues during formation of the M2, although some children begin consuming less $C_4$ sources than the previous period reflected by the PM1. The peak in dental defect formation at 3.7 years of age, coinciding with later crown mineralization of the PM1 and the beginning of formation of the M2 enamel, may indicate the shift to more $C_4$ sources in childhood resulted in greater physiological stress.

This notable contribution of $C_4$ foods in the childhood diet is not unique to the Near East or eastern Mediterranean. A $^{13}C$-enriched childhood diet also has been noted in studies of dental enamel carbonate in Dakhleh Oasis, Egypt (Dupras and Tocheri, 2007) and dentinal and bone collagen at Kulubnarti (Sandberg et al., 2014), where it has been attributed to breastmilk supplemented by millet gruel or milk from cows and goats who consumed millet or another $C_4$ crop. Millet has been found at Petra based on paleobotanical evidence although in minute amounts, but sorghum could have been used to sweeten foods in early childhood. The $C_4$ signature in childhood may derive from milk from $C_4$-consuming goats transported from areas with greater millet cultivation. The low levels of folic acid in goat milk compared to human milk unfortunately results in megaloblastic anemia due to folic acid deficiency if a child is fed primarily goat's milk from birth (O'Connor, 1994). The lack of infants and young children in this sample prevents determining the frequency of skeletal lesions related to this condition (cribra orbitalia and porotic hyperostosis) that may point to a reliance on goat's milk instead of human breastmilk. Furthermore, marine sources could potentially be used to supplement childhood diets in the form of fish meal or *garum* (fish sauce), but while adults were consuming marine sources at Petra, there is no evidence that children were doing so.

### *5.2. Diversity in water sources, catchment and storage practices, and food preparation*

The direction and magnitude of $\delta^{18}O$ value shifts across tooth classes varied greatly between individuals, suggesting the isotope ratio in children reflects fluctuations in drinking water source or food and water preparation rather than just the decline that occurs during weaning. Two out of three individuals with both an M1 and a PM1 do show an expected decline, and this decline is also seen between the PM1 and M2 in four individuals, which could indicate a shift in water source (mother vs. environmental) continued after formation of the PM1 but ceased before the M2 crown began mineralization. As noted above, this age of dental formation coincides with a peak in development of hypoplastic defects during childhood, indicating that this shift may have resulted in heightened physiological stress.

On the other hand, the data complexity suggests that $\delta^{18}O$ values instead are reflecting external factors such as one or more changes in water source during childhood, varied levels of non-human milk consumption, or cultural alteration through storage, heating, or fermentation. Not only do some individuals show an increase in $\delta^{18}O$ values by age of tooth crown formation, but the magnitude by which they increase or decrease varies by individual. These factors create increased diversity in $\delta^{18}O$ with age, with the M2s in the sample having a relatively high standard deviation than the other teeth. This increased heterogeneity suggests factors affecting $^{18}O$ enrichment in consumed water vary greatly within the population, such as animal milk supplementation, consumption of cooked foods or fermented products, or reliance on an array of water sources either across Petra or beyond if the individuals immigrated to the city.

Supplementation of human breastmilk with liquids more enriched in $^{18}O$, such as milk from grazing animals, would drive $\delta^{18}O$ higher (Daux et al., 2008). As noted above, milk from grazing animals consuming millet, a $C_4$ plant source, could explain the $C_4$-influenced childhood diet seen in the $\delta^{13}C$ data. Since milk from grazing animals is more enriched in $^{18}O$ than human breastmilk (Daux et al., 2008), children consuming animal milk would have notably higher $\delta^{13}C$ and $\delta^{18}O$ values. A positive linear relationship does not exist between these isotope ratios, and regional paleobotanical evidence from dung fuel has

found barley, a $C_3$ plant, to be the dominant grain used for animal fodder (Ramsay and Smith, 2013; Ramsay and Parker, 2016). Therefore, while some children may have been consuming animal milk during and after weaning, other factors were driving $\delta^{18}O$ values.

Children also may have an elevated $\delta^{18}O$ value due to drinking partially-evaporated water and/or through consuming cooked foods or fermented beverages. The preparation of gruel, pap, or spelt, foods recommended by ancient physicians for infants, would require heating of water within which the grains or bread were cooked. Water ingested via vegetables, meat, or other food products impact body water $\delta^{18}O$ less than that consumed as drinking water (Longinelli, 1984). However, experimental "stewing" of foods such as meat or legumes with vegetables, or even just boiling water on its own, resulted in a significant increase in $\delta^{18}O$ of the water used (Brettell et al., 2012). Petra was also a major vinicultural center (Bikai et al., 2008) and while cultural mores involving consumption of wine by breastfeeding women or children remain unclear, the process of fermentation through adding acid and/or sugar to grape juice increases the $\delta^{18}O$ of the resulting water in wine compared to the grape and the environmental water it relied on for growth (Akamatsu et al., 2019). Weaning infants and weaned children likely consumed prepared foods such as gruel or pap made from varied combinations of C3 and C4 grains according to the $\delta^{13}C$ values. The varied contribution of these foods to the diet could have resulted in divergence with age in $\delta^{18}O$ values.

In addition, Petra's unique hydrological system could have meant different families or households relied on water sources with distinct $\delta^{18}O$ signatures due to varied catchment and storage practices or to larger-range mobility. Seasonal rainfall in arid regions such as Petra is naturally enriched in $^{18}O$, and further enrichment occurs due to evaporation that varies due to surface temperature, ground cover, and humidity (Gat and Dansgaard, 1972). Thus, groundwaters in this environment likely are enriched in $^{18}O$ compared to precipitation than in less-arid regions. Precipitation catchment, water storage, irrigation, and other practices, particularly in dry months, can result in even more evaporation and thus enrichment in $^{18}O$. Petra inhabitants depended upon mixed combinations of groundwater from wells or springs, rainfall stored in cisterns, and or water that traveled across the landscape in aqueducts and irrigation channels, which could result in notable differences in $\delta^{18}O$. In addition, multi-year periods of climatic changes in temperature, rainfall, or humidity could further impact the $\delta^{18}O$ values of drinking water. While seasonal differences would be averaged in bulk enamel samples, a series of particularly wet or dry years would impact an infant's $\delta^{18}O$ signature. Relying on different regional sources due to mobility would similarly impact age-related shifts in $\delta^{18}O$ as well as result in increased heterogeneity within Petra. Other indicators of population mobility such as $^{87}Sr/^{86}Sr$ could identify whether unexpected $\delta^{18}O$ values or patterns resulted from migration.

### 5.3. Overall trends in childhood diet at Petra

Thus, not only does reliance on $C_3$ versus $C_4$ sources vary during childhood at Petra, but the water consumed by children either as drinking water, human or animal breastmilk, or in food has been differentially sourced, altered, and stored. This diversity exists early in childhood as depicted by the M1 isotope values, but increases with age, particularly during mineralization of the M2 crown. The neighborhood where those buried on the North Ridge lived cannot be confirmed by archaeological data, but textual evidence suggests the city's spaces were claimed by groups linked by lineage as well as trade or deity while the mortuary realm revolved more closely around kinship and lineage (Nehmé, 2013; Sachet, 2010). Therefore, there likely exists some parallel between neighborhood space and mortuary space, with most evidence pointing to the neighborhood surrounding the North Ridge tombs as the decedents' former places of residence. The isotope data by communal tomb identified some differences in variance as well as mean values between the tombs, with B.7 appearing to be the most divergent. However, no clear kin-based patterns in childhood feeding or water source could be identified. In fact, if these individuals were living in the same neighborhood or represent a small group of households one would expect them to have rather homogeneous $\delta^{18}O$ values reflecting a similar water source or catchment and storage practices, which is not the case. This may point to the important impact that cooking has on $\delta^{18}O$ in Petra children, and was a practice that differed within the community.

### 5.4. Isotopes and childhood stress and mortality

Childhood diet and water source or alteration patterns in infancy apparently are not associated with a greater or lesser chance of dying as a child. Therefore, following one track for feeding children and sourcing water had no more of an impact on childhood mortality than another. The inability to associate anterior teeth observed for hypoplastic defects and the premolars and molars used for stable isotope analysis does not allow assessment of childhood frailty and diet. In addition, the underrepresentation of infants and children in the sample masks the true age-at-death mortality pattern and children dying with conditions potentially leading to skeletal indicators of stress are invisible in the bioarchaeological record. This may explain the relatively lack of skeletal signs of active or survived episodes of physiological stress in the Petra sample.

The exploration of diet over childhood using bulk enamel samples may not provide clear evidence of weaning practices. However, in cases of poor collagen preservation they can illuminate the extent that diet as reflected in $\delta^{13}C$ and factors affecting $^{18}O$ enrichment vary, even within hypothesized kin groups. Although this assemblage is mostly commingled, general links with other indicators of childhood morbidity and mortality can be explored. The Petra community buried in the North Ridge tombs did not follow a set of practices in terms of childhood diet or food preparation. However, the diverse practices did result in differential childhood stress or mortality. Intra-community variation in childhood feeding behaviors is not uncommon, and often fluctuates based on personal choice, socioeconomic factors such as employment or involvement in a trade, physiological factors such as health of mother and breastmilk availability, or presence of other nursing infants in the household (e.g., Stuart-Macadam and Dettwyler, 1995; Tomori et al., 2017; Wright, 2013). Variation within these tombs could also reflect temporal shifts regarding childhood diet over the 200 years that they were in use.

## 6. Conclusions

This combined approach using $\delta^{13}C$ and $\delta^{18}O$ from bulk dental enamel carbonate to illuminate the variety of foods included in the childhood diet and diversity in water sources, catchment, and alteration through cooking or other anthropogenic processes has provided a unique perspective of childhood in Petra. Children were provided a higher proportion of $C_4$ foods during weaning and postweaning than what adults consumed, although this varied from child to child especially during 3.7 to 7.4 years, during formation of the M2 crown. This could represent a period of greater childhood autonomy regarding subsistence or simply a shift to a more varied adult diet as represented by the bone apatite data. However, the peak in dental hypoplastic defects at 3.7 years may suggest this also was a period of heightened physiological stress. The age-related increase in dietary variation is mirrored by greater heterogeneity in variables affecting $^{18}O$ enrichment, with food preparation or mobility being the likeliest factors. Exploring migration through other isotopes could clarify the unexpected patterns in $\delta^{18}O$ with age. Dental enamel microstructure could provide a better indicator of childhood frailty in these teeth (Temple et al., 2012), although the extent of occlusal wear in this sample may prevent a large-scale study. The variables affecting $\delta^{18}O$ nor $\delta^{13}C$ values also do not impact childhood mortality, but truly characterizing their effect on life history at

Petra may be hindered by the commingled nature of this assemblage.

## Acknowledgments

The Petra North Ridge Project, co-directed by Megan Perry and S. Thomas Parker, was funded largely by the National Endowment for the Humanities (NEH Collaborative Grant RZ-5155-13), the National Geographic Society Committee for Research and Exploration (#9831-16), the American Center of Oriental Research, al-Himma Foundation, East Carolina University, North Carolina State University, and SUNY Brockport. Gratitude goes to the Department of Antiquities of Jordan for collaboration in the field project and allowing exportation and destructive analysis of the samples. We also would like to thank ECU Anthropology graduate students Michael Navarro, Cori Taylor, Liz Salcito, and Elizabeth Young for running the FTIR-ATR analyses, and for Dr. Jack Pender of ECU's Department of Chemistry for providing access to the spectrometer.

## References

Akamatsu, F., Shimizu, H., Kamada, A., Igi, Y., Fuji, T., Goto-Yamamoto, N., 2019. Increase in the oxygen stable isotopic composition of water in wine with low ethanol yield. Nat. Sci. Rep. 9, 11039.

Beasley, M.M., Bartelink, E.J., Taylor, L., Miller, R.M., 2014. Comparison of transmission FTIR, ATR, and DRIFT spectra: implications for assessment of bone bioapatite diagenesis. J. Archaeol. Sci. 46, 16–22.

Beaumont, J., Atkins, E., Buckberry, J., Haydock, H., Horne, P., Howcroft, R., et al., 2018. Comparing apples and oranges: why infant bone collagen may not reflect dietary intake in the same way as dentine collagen. Am. J. Phys. Anthropol. 167, 524–540.

Beaumont, J., Gledhill, A., Lee-Thorp, J., Montgomery, J., 2013. Childhood diet: a closer examination of the evidence from dental tissues using stable isotope anlaysis of incremental human dentine. Archaeometry 55, 277–295.

Beaumont, J., Montgomery, J., Buckberry, J., Jay, M., 2015. Infant mortality and isotopic complexity: New approaches to stress, maternal health, and weaning. Am. J. Phys. Anthropol. 157, 411–457.

Beckers, B., Schütt, B., Tsukamoto, S., Frechen, M., 2013. Age determination of Petra's engineered landscape – optically stimulated luminescence (OSL) and radiocarbon ages of runoff terrace systems in the Eastern Highlands of Jordan. J. Archaeol. Sci. 40, 333–348.

Bikai, P.M., Kanellopoulos, C., Saunders, S.L., 2008. Beidha in Jordan: a Dionysian hall in a Nabataean landscape. Am. J. Archaeol. 112, 465–507.

Bikai, P.M., Perry, M.A., 2001. Petra North Ridge Project Tombs 1 and 2: preliminary report. Bull. Am. Sch. Orien. Res. 104, 59–78.

Bouchaud, C., 2015. Agrarian legacies and innovations in the Nabataean territory. ArcheoSciences 39, 103–124.

Bourbou, C., Garvie-Lok, S.J., 2009. Breastfeeding and weaning patterns in Byzantine times. In: Papaconstantinou, A., Talbot, A.-M. (Eds.), Becoming Byzantine: Children and childhood in Byzantium. Dumbarton Oaks, Washington, DC, pp. 65–83.

Brettell, R., Montgomery, J., Evans, J., 2012. Brewing and stewing: the effect of culturally mediated behaviour on the oxygen isotope composition of ingested fluids and the implications for human provenance studies. J. Anal. At. Spectrom. 27, 778–785.

Brooks, S.T., Suchey, J.M., 1990. Skeletal age determination based on the os pubis: a comparison of the Acsadi-Memskeri and Suchey-Brooks methods. Human Evol. 5, 227–238.

Budd, P., Montgomery, J., Barreiro, B., Thomas, R.G., 2000. Differential diagenesis of strontium in archaeological human dental tissues. Appl. Geochem. 15, 687–694.

Canipe, C., 2014. Exploring Quality of Life at Petra through Paleopathology. M.A. Thesis, Department of Anthropology, East Carolina University.

Buikstra, J.E., Ubelaker, D.H., 1994. Standards for Data Collection from Human Skeletal Remains. Arkansas Archaeological Survey, Fayetteville, AR.

Dal Sasso, G., Lebon, M., Angelini, I., Maritan, L., Usai, D., Artioli, G., 2016. Bone diagenesis variability among multiple burial phases at Al Khiday (Sudan) investigated by ATR-FTIR spectroscopy. Palaeogeogr. Palaeoclimatol. Palaeoecol. 463, 168–179.

DeNiro, M., 1985. Postmortem preservation and alteration of *in vivo* bone collagen isotope ratios in relation to palaeodietary reconstruction. Nature 317, 806–809.

DeNiro, M.J., Epstein, S., 1978. Influence of diet on the distribution of carbon isotopes in animals. Geochim. Cosmochim. Acta 42, 495–506.

Dupras, T.L., Tocheri, M.W., 2007. Reconstructing infant weaning histories at Roman Period Kellis, Egypt using stable isotope analysis of dentition. Am. J. Phys. Anthropol. 134, 63–74.

Dupras, T.L., Schwarcz, H.P., Fairgrieve, S.I., 2001. Infant feeding and weaning practices in Roman Egypt. Am. J. Phys. Anthropol. 115, 204–212.

Dupras, T.L., Schwarcz, H.P., 2001. Strangers in a strange land: stable isotope evidence for human migration in the Dakhleh Oasis. Egypt. J. Archaeol. Sci. 28, 1199–1208.

Fuller, B.T., Fuller, J.L., Harris, D.A., Hedges, R.E.M., 2006. Detection of breastfeeding and weaning in modern human infants with carbon and nitrogen stable isotope ratios. Am. J. Phys. Anthropol. 129, 279–293.

Gat, J.R., Dansgaard, W., 1972. Stable isotope survey of the fresh water occurrences in Israel and the northern Jordan rift valley. J. Hydrol. 16, 177–212.

Gluckman, P.D., Cutfield, W., Hofman, P., Hanson, M.A., 2005. The fetal, neonatal, and infant environments—the long-term consequences for disease risk. Early Human Dev. 81, 51–59.

Goodman, A.H., Armelagos, G., 1988. Childhood stress, cultural buffering, and decreased longevity in a prehistoric population. Am. Anthropol. 90, 936–944.

Goodman, A.H., Rose, J.C., 1990. Assessment of systemic physiological perturbations from dental enamel hypoplasias and associated histological structures. Yearbook Phys. Anthropol. 33, 59–110.

Gordon, C.C., Buikstra, J.E., 1981. Soil pH, bone preservation, and sampling bias at mortuary sites. Am. Antiq. 48, 566–571.

Gowland, R.L., 2015. Entangled lives: Implications of the developmental origins and health and disease hypothesis for bioarchaeology and the life course. Am. J. Phys. Anthropol. 158, 530–540.

Gregoricka, L.A., Sheridan, S.G., 2017. Continuity or conquest? A multi-isotope approach to investigating identity in the Early Iron Age of the Southern Levant. Am. J. Phys. Anthropol. 162, 73–89.

Guy, H., Massett, C., Baud, C., 1997. Infant taphonomy. Int. J. Osteoarchaeol. 7, 221–229.

Halcrow, S., King, C., Millard, A., Snoddy, A., Scott, R., Elliott, G., et al., 2017. Out of the mouth of babes and sucklings: breastfeeding and weaning in the past. In: Tomori, C., Palmquist, A., Quinn, E. (Eds.), Breastfeeding: New anthropological approaches. Routledge, London, pp. 155–169.

Halcrow, S., Tayles, N., 2011. The bioarchaeological investigation of children and childhood. Blackwell, London, pp. 333–360.

Halcrow, S., Tayles, N., 2008. The bioarchaeological investigation of childhood and social ages: problems and prospects. J. Archaeol. Method Theory 15, 190–215.

Harbeck, M., Grupe, G., 2009. Experimental chemical degradation compared to natural diagenetic alteration of collagen: implications for collagen quality indicators for stable isotope analysis. Archaeol. Anthropol. Sci. 1, 43–57.

Hedges, R.E.M., 2002. Bone diagenesis: an overview of processes. Archaeometry 44, 319–328.

Hedges, R.E.M., Millard, A.R., 1995. Bones and groundwater: towards the modelling of diagenetic processes. J. Archaeol. Sci. 22, 155–164.

Henriquez, A.C., Oxenham, M.F., 2019. New distance-based exponential regression method and equations for estimating the chronology of linear enamel hypoplasia (LEH) defects on the anterior dentition. Am. J. Phys. Anthropol. 168, 510–520.

Hillson, S., 2014. Tooth Development in Human Evolution and Bioarchaeology. Cambridge University Press, Cambridge.

Hollund, H.I., Ariese, F., Fernandes, R., Jans, M.M.E., Kars, H., 2013. Testing an alternative high-throughput tool for investigating bone diagenesis: FTIR in attenuated total reflection (ATR) mode. Archaeometry 55, 507–532.

Hoppe, K.A., Koch, P.L., Furutani, T.T., 2003. Assessing the preservation of biogenic strontium in fossil bones and tooth enamel. Int. J. Osteoarchaeol. 20–28.

Katzenberg, M.A., Herring, D.A., Saunders, S.R., 1996. Weaning and infant mortality: evaluating the skeletal evidence. Am. J. Phys. Anthropol. 39, 177–199.

Kendall, E., 2016. The "terrible tyranny of the majority": recognising population variability and individual agency in past infant feeding practices. In: Powell, L., Southwell-Wright, W., Gowland, R. (Eds.), Care in the Past: archaeological and interdisciplinary perspectives. Oxbow Books, Oxford, pp. 39–51.

King, C.L., Millard, A.R., Grocke, D.R., Standen, V.G., Arriaza, B.T., Halcrow, S.E., 2017. A comparison of using bulk and incremental isotopic anlayses to establish weaning practices in the past. STAR: Sci. Technol. Archaeol. Res. 3, 126–134.

Krueger, H.W., Sullivan, C.H., 1984. Models for carbon isotope fractionation between diet and bone, in: Stable Isotopes in Nutrition, Turnlund, J.R. and Johnson, P.E. (Eds.), American Chemical Society Symposium Series v. 258, pp. 205-220.

Laskaratos, J., Poulakou-Rebelakou, E., 2003. Oribasius (Fourth Century) and Early Byzantine perinatal nutrition. J. Pediatr. Gastroenterol. Nutr. 16, 186–189.

Lebon, M., Reiche, I., Gallet, X., Bellot-Gurlet, L., Zazzo, A., 2016. Rapid quantification of bone collagen content by ATR-FTIR spectroscopy. Radiocarbon 58, 131–145.

Lee-Thorp, J., Sponheimer, M., 2003. Three case studies used to reassess the reliability of fossil bone and enamel isotope signals for paleodietary studies. J. Anthropol. Archaeol. 22, 208–216.

Lee-Thorp, J.A., Sealy, J.C., van der Merwe, N.J., 1989. Stable carbon isotope differences between bone collagen and bone apatite, and their relationship to diet. J. Archaeol. Sci. 16, 585–599.

Lewis, M.E., 2007. The Bioarchaeology of Children. Cambridge University Press, Cambridge.

Longinelli, A., 1984. Oxygen isotopes in mammal bone phosphate: a new tool for paleohydrological and paleoclimatological research? Geochim. Cosmochim. Acta 48, 385–390.

Lovejoy, C.O., Meindl, R.S., Pryzbeck, T.R., Mensforth, R.P., 1985. Chronological metamorphosis of the auricular surface of the ilium: a new method for the determination of adult skeletal age at death. Am. J. Phys. Anthropol. 68, 15–28.

Luz, B., Kolodny, Y., Horowitz, M., 1984. Fractionation of oxygen isotopes between mammalian bone-phosphate and environmental water. Geochim. Cosmochim. Acta 48, 1689–1693.

Manolis, S.K., Eliopooulos, C., Koilias, C.G., Fox, S.C., 2009. Sex determination using metacarpal biometric data from the Athens Collection. Forensic Sci. Int. 193, 130.e1–130.e6.

Masterson, E.E., Fitzpatrick, A.L., Enquobahrie, D.A., Manci, L.A., Conde, E., Hujoel, P.P., 2017. Malnutrition-related early childhood exposures and enamel defects in the permanent dentition: a longitudinal study from the Bolivian Amazon. Am. J. Phys. Anthropol. 164, 416–423.

Matsubayashi, J., Tayasu, I., 2019. Collagen turnover and isotopic records in cortical bone. J. Archaeol. Sci. 106, 37–44.

Mays, S., 2010. The effects of infant weeding practices on infant and maternal health in a Medieval community. Childhood in the Past, 63–78.

Moorees, C.F.A., Fanning, E.A., Hunt, E.E., 1963. Age variation of formation stages for ten

permanent teeth. J. Dent. Res. 42, 1490–1502.
Mountrakis, C., Eliopoulos, C., Koilias, C.G., Manolis, S.K., 2010. Sex determination using metatarsal osteometrics from the Athens collection. Forensic Sci. Int. 200, 178.e1–178.e7.
Nehmé, L., 2013. The installation of social groups in Petra. In: Mouton, M., Schmid, S.G. (Eds.), Men on the Rocks: The Formation of Nabataean Petra. Logos Verlag GmbH, Berlin, pp. 113–128.
Nielsen-Marsh, C.M., Hedges, R.E.M., 2000. Patterns of diagenesis in bone I: the effects of site environments. J. Archaeol. Sci. 27, 1139–1150.
O'Connor, D.L., 1994. Folate in goat milk products with reference to other vitamins and minerals: a review. Small Ruminant Res. 14, 143–149.
Ortloff, C.R., 2005. The water supply and distribution system of the Nabataean city of Petra (Jordan), 300 BC - AD 300. Cambridge Archaeol. J. 15, 93–109.
Osterholtz, A.J., 2019. Advances in documentation of commingled and fragmentary remains. Adv. Archaeol. Practice 7, 77–86.
Parker, S.T., Perry, M.A., 2017. The Petra North Ridge Project: 2014 season. Annual of the Department of Antiquities of Jordan, 58, 287-302.
Parker, S.T., Perry, M.A., 2013. Petra North Ridge Project: The 2012 Season. Annual of the Department of Antiquities of Jordan, 57, 399-407.
Pearson, J.A., Hedges, R.E.M., Molleson, T.I., Ozbek, M., 2010. Exploring the relationship between weaning and infant mortality: An isotope case study from Aşıklı Höyük and Çayönü Tepesi. Am. J. Phys. Anthropol. 143, 448–457.
Perry, M.A., 2017. Sensing the Dead: Mortuary Ritual and Tomb Visitation at Nabataean Petra. Syria 94, 99–106.
Perry, M.A., Walker, J.L., 2018. The Nabataean Way of Death on Petra's North Ridge. In: Eger, C., Mackensen, M. (Eds.), Death and Burial in the Near East from Roman to Islamic Times. Reichert Verlag, Weisbaden, pp. 121–137.
Perry, M.A., Coleman, D., Dettman, D.L., al-Shiyab, A.H., 2009. An isotopic perspective on the transport of Byzantine mining camp laborers into southwestern Jordan. Am. J. Phys. Anthropol. 140, 429–441.
Phenice, T., 1969. A newly developed visual method of sexing in the os pubis. Am. J. Phys. Anthropol. 30, 297–301.
Prowse, T., Schwarcz, H.P., Garnsey, P., Knyf, M., Macchiarelli, R., Bondioli, L., 2007. Isotopic evidence for age-related immigration to Imperial Rome. Am. J. Phys. Anthropol. 132, 510–519.
Ramsay, J., Bedal, L., 2015. Garden variety seeds? Botanical remains from the Petra Garden and Pool Complex. Veg. Hist. Archaeobot. 24, 621–634.
Ramsay, J.H., Parker, S.T., 2016. A diachronic look at the agricultural economy at the Red Sea port of Aila: an archaeobotanical case for hinterland production in arid environments. Bull. Am. Sch. Orien. Res. 376, 101–120.
Ramsay, J., Smith II, A.M., 2013. Desert agriculture at Bir Madhkur: the first archaeobotanical evidence to support the timing and scale of agriculture during the Late Roman/Byzantine period in the hinterland of Petra. J. Arid Environ. 99, 51–63.
Reid, D.J., Dean, M.C., 2006. Variation in modern human enamel formation times. J. Hum. Evol. 50, 329–346.
Reid, D.J., Dean, M.C., 2000. The timing of linear hypoplasias on human anterior teeth. Am. J. Phys. Anthropol. 113, 135–139.
Richards, M.P., Mays, S., Fuller, B.T., 2002. Stable carbon and nitrogen isotope values of bone and teeth reflect weaning age at the Medieval Wharram Percy site, Yorkshire, UK. Am. J. Phys. Anthropol. 119, 205–210.
Sachet, I., 2010. Feasting with the dead: funerary marzeah in Petra, in: Death and Burial in Arabia and Beyond: Multidisciplinary Perspectives. Archaeopress, Oxford, pp. 249–262.
Sandberg, P.A., Sponheimer, M., Lee-Thorp, J., Van Gerven, D., 2014. Intra-tooth stable isotope analysis of dentine: a step toward addressing selective mortality in the reconstruction of life history in the archaeological record. Am. J. Phys. Anthropol. 155, 281–298.
Saunders, S.R., 1992. Subadult skeletons and growth related studies. In: Saunders, S.R., Katzenberg, M.A. (Eds.), Skeletal Biology of Past Peoples: Research Methods. Wiley-Liss, New York, pp. 1–20.
Schmid, S., 2002. The International Wadi Farasa Project (IWFP): 2001 Season. Annual of the Department of Antiquities of Jordan, 46, 257–277.
Schurr, M.R., 1998. Using stable nitrogen-isotopes to study weaning behavior in past populations. World Archaeol. 30, 327–342.
Šešelj, M., Sherwood, R.J., Kongisberg, L.W., 2019. Timing of development of the permanent mandibular dentition: new reference values from the Fels Longitudinal Study. The Anatomical Record, https://doi.org/10.1002/ar.24108.
Sillen, A., 1989. Diagenesis of the inorganic phase of coritical bone. Cambridge University Press, Cambridge, pp. 211–229.
Slovak, N., Paytan, A., Wiegand, B.A., 2009. Reconstructing Middle Horizon mobility patterns on the coast of Peru through strontium isotope analysis. J. Archaeol. Sci. 36, 157–165.
Spradley, M.K., Jantz, R.L., 2011. Sex estimation in forensic anthropology: skull versus postcranial elements. J. Forensic Sci. 56, 289–296.
Stathopoulou, E.T., Psycharis, V., Chryssikos, G.D., Gionis, V., Theodorou, G., 2008. Bone diagenesi: new data from infrared spectroscopy and x-ray diffraction. Palaeogeogr. Palaeoclimatol. Palaeoecol. 266, 168–174.
Stojanowski, C., 1999. Sexing potential of fragmentary and pathological metacarpals. Am. J. Phys. Anthropol. 109, 245–252.
Stuart-Macadam, P., Dettwyler, K., 1995. Breast-feeding: Biocultural perspectives. DeGruyter, New York.
Studer, J., 2007. Animal exploitation in the Nabataean world, in: The World of the Nabataeans. Volume 2 of the International Conference The World of the Herods and the Nabataeans held at the British Museum, 17-19 April 2001, Politis, K.D. (Ed.), Franz Steiner Verlag, Stuttgart, pp. 251–272.
Temple, D.H., Nakatsukasa, M., McGroarty, J.N., 2012. Reconstructing patterns of systemic stress in a Jomon period subadult using incremental mirostructures of enamel. J. Archaeol. Sci. 39, 1634–1641.
Thompson, J.U., Gauthier, M., Islam, M., 2009. The application of a new method of Fourier transform infrared spectroscopy to the analysis of burned bone. J. Archaeol. Sci. 36, 910–914.
Tomori, C., Palmquist, A., Quinn, E., 2017. Introduction: Towards new anthropologies of breastfeeding, in: Breastfeeding: New anthropological approaches, Anonymous Routledge, London, pp. 1–25.
Tsutaya, T., Yoneda, M., 2015. Reconstruction of breastfeeding and weaning practices using stable isotope and trace element analyses: a review. Yearbook Phys. Anthropol. 156, 2–21.
Tuross, N., 2002. Alteration in fossil collagen. Archaeometry 44, 427–434.
Tuross, N., Reynard, L.M., Harvey, E., Coppa, A., McCormick, M., 2017. Human skeletal development and feeding behavior: the impact on oxygen isotopes. Archaeol. Anthropol. Sci. 9, 1453–1459.
Tykot, R.H., 2018. Bone chemistry and ancient diet, in: Encyclopedia of Global Archaeology, 2nd edition, Smith, C. (Ed.), doi:10.1007/978-3-319-51726-1_329-2.
Tykot, R.H., 2014. Bone chemistry and ancient diet, in: Encyclopedia of Global Archaeology, Smith, C. (Ed.), Springer, pp. 931-941.
Tykot, R.H., 2004. Stable Isotopes and Diet: You Are What You Eat. Società Italiana di Fisica, Bologna, pp. 433–444.
Daux, V., Lécuyer, C., Héran, M., Amiot, R., Simon, L., Fourel, F., et al., 2008. Oxygen isotope fractionation between human phosphate and water revisited. In: J. Human Evol. 55. pp. 1138–1147.
Victora, C., Bahl, R., Barros, A., Franca, G., Horton, S., Krasevec, J., et al., 2016. Breastfeeding in the 21st century: epidemiology, mechanisms, and lifelong effect. In: Lancet 387. pp. 475–490.
Walker, P.L., Johnson, J.R., Lambert, P.M., 1988. Age and sex biases in the preservation of human skeletal remains. Am. J. Phys. Anthropol. 76, 183–188.
Weiner, S., Bar-Yosef, O., 1990. States of preservation of bones from prehistoric sites in the Near East: a survey. J. Archaeol. Sci. 17, 187–196.
Wood, J.W., Milner, G.R., Harpending, H.C., Weiss, K.M., 1992. The osteological paradox: problems in inferring prehistoric health from skeletal samples. Curr. Anthropol. 33, 348–358.
World Health Organization, 2003. Global Strategy for Infant and Young Child Feeding. World Health Organization, Geneva.
Wright, L.E., 2013. Examining childhood diets at Kaminaljuyu, Guatemala, through stable isotopic analysis of sequential enamel microsamples. Archaeometry 55, 113–133.
Wright, L.E., Schwarcz, H.P., 1999. Correspondence between stable carbon, oxygen, and nitrogen isotopes in human tooth enamel and dentine: infant diets at Kaminlajuyu. J. Archaeol. Sci. 26, 1159–1170.
Wright, L.E., Schwarcz, H.P., 1996. Infrared and isotopic evidence for diagenesis of bone apatite at Dos Pilas, Guatemala: palaeodietary implications. J. Archaeol. Sci. 23, 933–944.
Wright, L.E., Schwarcz, H.P., 1998. Stable carbon and oxygen isotopes in human tooth enamel: identifying breastfeeding and weaning in prehistory. Am. J. Phys. Anthropol. 106, 1–18.